ROYAL SOCIETY
OF CHEMISTRY

PAPER

Check for updates

Flexible superhydrophobic surfaces with condensate microdrop self-propelling functionality based on carbon nanotube films†

Xiaojing Gong, [ID] *[a] Jing Xu,[a] Zhenzhong Yong*[b] and Seeram Ramakrishna*[c]

With the development of flexible electronics and wearable devices, there is strong demand for flexible, superhydrophobic, and multifunctional coatings. Motivated by the promise of attractive multifaceted functionality, various techniques have been developed to fabricate flexible surfaces with non-wetting properties. However, until now, there have been few reports on superhydrophobic surfaces with condensate microdrop self-propelling (CMDSP) functionality on a carbon nanotube film. Here, we used a facile electrodeposition method to develop for the first time a new type of flexible superhydrophobic surface with CMDSP functionality based on carbon nanotube films. These flexible CMDSP surfaces are robust after multiple cycles of bending of the film-coated substrate, *i.e.*, without impacting the surface superhydrophobicity and CMDSP performance. The proposed light and flexible surface, combined with CMDSP, will support a novel generation of coatings that are multifunctional, flexible, smart, and energy saving. This new type of functional flexible interface not only opens new avenues in research into the fundamental structure–property relationships of materials, but also exhibits significant application potential for advanced technologies.

1. Introduction

By appropriately designing and engineering surfaces with different nanostructures, a large variety of multifunctional composite materials can be created for a wide range of application areas, from chemistry to advanced biomedical science. Currently, a new type of superhydrophobic surface is attracting interest due to its condensate microdrop self-propelling (CMDSP) functionality on metal, silicon, or other rigid substrates.[1,2] Different from conventional superhydrophobic surfaces characterized by gravity-driven shedding or bouncing of macroscopic water drops, such novel surfaces can self-remove small-scale condensate microdrops as they jump away *via* coalescence-released excess surface energy. This phenomenon does not require other forces such as gravity or stream shear force; thus, the surfaces retain their robust super-hydrophobicity under moisture, condensation, or steam conditions.[3–10] CMDSP surfaces are considered to have significant value in applications such as self-cleaning of moisture,[11] electrostatic energy harvesting,[12] and enhanced condensation heat transfer[13] for higher efficiency energy utilization and thermal management.

Typically, the building of special surficial nanostructures is needed to obtain CMDSP functionality.[14–17] There is a prototype in nature. Wisdom *et al.*[18] reported that tiny condensate microdrops on the closely packed nanocone surface of cicada wings can self-remove by jumping *via* mutual coalescence; thus, the surface has a moisture self-cleaning function. Based on this bio-inspiration, many studies have shown that constructing arrays of inorganic nanostructures with sharp tips can indeed endow the surfaces with CMDSP functionality. In principle, any sub-microscale structures with a small feature size (*i.e.*, tip size and interspace) and a certain height (or depth) can become effective candidates for creating CMDSP surfaces. Such structures are arrays of closely packed nanotips, such as nanocones,[19–22] nanoneedles,[23–26] nanopencils,[13] tip-like nanotubes,[2,27] and nanorod-capped nanopores,[16,28] as well as the porous structure of nanoparticles,[15] nanosheets[4,12,29,30] on copper substrates, nanowires,[31,32] and two-tier structures on

[a]*Institute of Materials Science and Engineering, National Experimental Demonstration Center for Materials Science and Engineering, Changzhou University, Changzhou, 213164, P. R. China*

[b]*Division of Advanced Nanomaterials, Suzhou Institute of Nano-Tech and Nano-Bionics, Chinese Academy of Sciences, Suzhou, 215123, P. R. China*

[c]*Center for Nanofibers and Nanotechnology, National University of Singapore, 117576, Singapore*

† Electronic supplementary information (ESI) available: Movie 1: Water drops adhering on the up-bent surfaces of pristine CNTF. Movie 2: Water drops adhering on the down-bent surfaces of pristine CNTF. Movie 3: Water drops jumping off the up-bent surfaces of the ZnO nanoneedles–CNT composite film. Movie 4: Water drops jumping off the down-bent surfaces of the ZnO nanoneedles–CNT composite film. Movie 5: Water drops jumping off the continuous up and down bent surfaces of the ZnO nanoneedles–CNT composite film. Movie 6: CMDSP phenomenon on flat surfaces of the ZnO nanoneedles–CNT composite film. Movie 7: Durability of superhydrophobicity after rubbing. Movie 8: Durability of superhydrophobicity after scratching. See DOI: 10.1039/d0na00477d

silicon substrates.[33,34] Despite much effort made to date, most nanostructures are constructed on rigid inorganic or metal substrates, *i.e.*, few flexible CMDSP surfaces have been reported.

However, there have been several reports about flexible superhydrophobic surfaces based on polymers.[35–37] These flexible superhydrophobic surfaces lack the CMDSP functionality, which limits their application in the areas of moisture self-cleaning, energy utilization, and thermal management. Despite there being some polymer CMDSP surfaces, the substrates are rigid glass, and several steps are required to obtain sharp polymer tips.[11] Furthermore, as most flexible polymers are not conductors, it is difficult to use the facile electrodeposition method to construct nanotip structures on these flexible surfaces. Another promising flexible material is called nanocellulose paper, but this material has poor shape stability in water and other solutions and a low decomposition temperature (320 °C).[38] Hence, the successful fabrication of robust superhydrophobic surface nanostructures with CMDSP functionality on a suitable flexible substrate using facile one-step methods is very appealing but remains a challenge.

In this work, we make a breakthrough to show, for the first time, the fabrication of flexible CMDSP surfaces. We find that zinc oxide (ZnO) nanoneedles can endow flexible carbon nanotube films (CNTFs) with CMDSP functionality when fabricated using a facile and cheap electrodeposition method. CNTFs consist of carbon nanotubes that can sustain their flexibility even at low temperatures. They are good conductors if composed of metal CNTs. However, prior to our study, there were no reports on constructing nanoneedles on CNTFs by electrodeposition. One of the greatest challenges to overcome is that these carbon assemblies are easily dispersed in an electrolyte during the electrodeposition process. We pre-treated the CNTF using an efficient microwave method to strengthen the film and avoid dispersion during the electrodeposition process. Our results show that the ZnO–CNTF composite film can maintain its flexibility even after it is covered with rigid nanoneedles. The composite film is very robust and retains its superhydrophobicity, even after continuous up-and-down bending. Furthermore, due to the microscopically low-adhesive nature of its building blocks, the flexible composite film has been endowed with CMDSP functionality, which can not only realize high-density nucleation but also maintain the high frequency of self-propelled jumping. These findings helped in the development of novel flexible coatings with moisture self-cleaning, stretchable electrodes, and advanced heat and mass transfer nanomaterials and devices.

2. Experimental section

2.1 Materials fabrication

Carbon nanotube films. CNT films were prepared by a floating catalyst chemical vapor deposition method. An ethanol solution with 2 wt% ferrocene and 1 vol% thiophene was injected into a tube reactor using a programmable syringe injector, which was used as the carbon source and catalyst for CNT growth. Hydrogen (2000 sccm) was injected as the carrier gas. The growth of CNTs was performed at about 1200 °C.[39]

Carbon nanotubes were organized inside of the tube as a thin aerogel hollow tube, and then flowed out of the reactor tube with the help of flowing gases. We then densified the sheet, followed by continuously collecting the film on a mandrel. In order to prevent the CNT films from becoming rotten from liquid logging, we utilized microwave treatment to strengthen the CNT films.

Electrodeposition of ZnO nanoneedles on carbon nanotube films. A thin Zn film was electrodeposited on the surface of pre-treated CNT film in an aqueous solution of 0.1 M KCl and 0.2×10^{-3} M $ZnCl_2$ for 5 min at a potential of −1.8 V. Subsequently, aligned ZnO nanoneedles can be obtained *via* immersing the Zn-electroplated surfaces of copper blocks in an aqueous solution of 4 M NaOH and 0.5 M $Zn(NO_3)_2 \cdot 6H_2O$ at 60 °C for varied growth time.[40]

Surface modifications. After rinsing with water and drying in a nitrogen air flow, all nanostructure samples were modified with low-surface-energy fluorosilane. Samples were placed, together with a cup containing 10 μL heptadeca-fluorodecyltrimethoxy silane (Shin-Etsu Chemical Co., Ltd., Japan), into a glass container. The container was sealed with a cap and then heated for 2 h at 120 °C.[40]

2.2 Characterization

The surface morphologies of *in situ* grown nanocones were observed *via* scanning electron microscopy (SEM, Phenom proX, Holland). Their element composition was analyzed using an EDAX X-ray energy-dispersive spectrometer (EDS) coupled with the SEM. A high-speed microscopic imaging system (Keyence VHX-6000, Japan) was used for studying the dynamic condensation behaviors of the sample surfaces under magnifications of 50× and 500× with frame rates of 50 F s^{-1}. The samples were fastened on a horizontally placed cooling stage (*ca.* 2 °C) in a controlled environment with an ambient temperature of *ca.* 25 °C and relative humidity of *ca.* 85%.

3. Results and discussion

To achieve the desired CMDSP functionality, it is necessary to minimize the dissipation of coalescence-released excess surface energy caused by solid–liquid adhesion.[25] According to previous research,[40] nanoneedles have an extremely low solid–liquid interface adhesion and can endow surfaces with the CMDSP functionality. Hence, based on our recent work in constructing nanostructures on CNTF,[41] we first design the flexible CMDSP film consisting of ZnO nanoneedles and CNTF. Fig. 1 shows the macroscopic and microscopic structures, together with the function of our ZnO nanoneedle and CNTF composite films. The lower image of Fig. 1 depicts our design for a ZnO–CNTF composite nanosurface. After fluorosilane modification, the water droplets can self-propel on the surface, driven by coalescence-released excess surface energy. The gray film, green cones, and blue circles represent CNTF, ZnO nanoneedles, and water droplets, respectively. The upper images show more atomic details of how CNTs assemble into bundles and bundles pack into fibers. The growth details are also shown, *i.e.*, zinc and
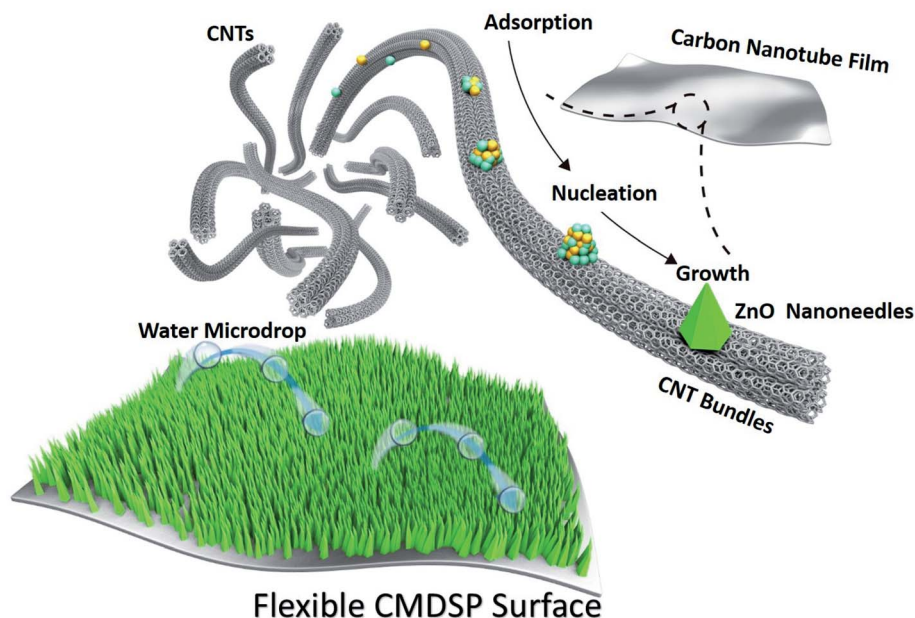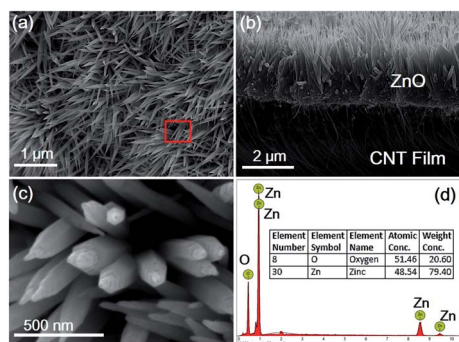
Fig. 1 Schematic showing the utilization of ZnO nanoneedles (green cones) to endow flexible CNTF surfaces (gray film) with a condensate microdrop self-propelling function. As shown by the lower images, water microdrops (blue circles) jump on the tips of ZnO nanoneedles. The upper images show that the flexible CNT films consist of CNTs. During the electrodeposition process, adatoms (yellow and blue balls) first adsorb on the surfaces of CNT bundles, and then they nucleate and grow into ZnO nanoneedles.
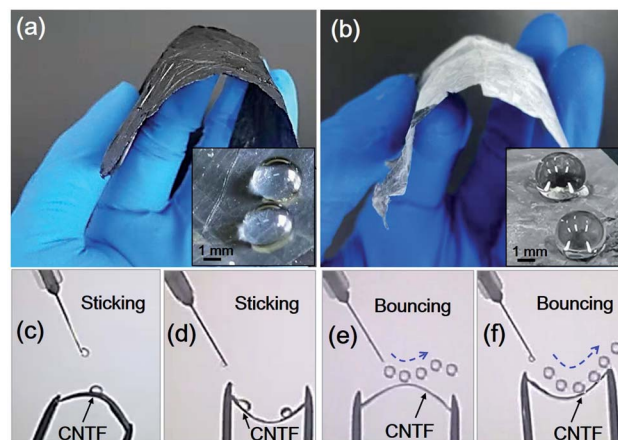
oxygen adatoms adsorb, nucleate on surfaces of CNT bundles, and then grow into ZnO nanoneedles on CNT bundles. The next issues to be addressed are the growth of ZnO nanoneedle coatings on the flexible CNTF surface by using the facile, low-cost, and scalable electrodeposition method and verification of their functional utility.

It has been reported that electrodeposited ZnO nanoneedle films can be rapidly grown on copper or silicon surfaces. However, there have been no reports of electrodeposited ZnO nanoneedles on top of CNTF or their use for studying CMDSP functionality. One big challenge is that these carbon assemblies are easily dispersed in electrolyte during the electrodeposition process. Here, in order to successfully grow ZnO nanoneedles on CNTF surfaces, we first apply a microwave pretreatment to strengthen the CNTFs so they avoid dispersion during a 30 min

electrodeposition process. Then, we use the facile electrodeposition method to deposit ZnO nanoneedles on CNTFs. Fig. 2a and b show typical scanning electron microscopy (SEM) top and side views of the as-grown nanoneedles, corresponding to

Fig. 3 Comparison of pristine and nanoneedle-covered CNTFs in terms of their flexibility and superhydrophobicity at the macroscale level. (a) Flexible pristine CNTF. (b) Flexible nanoneedle-covered CNTF. The insets show optical images of macroscale drops (∼3 mm in diameter) on the surface of pristine CNTF and nanoneedle-covered CNTF, respectively. (c–f) Overlapped optical images showing continuous macroscale drops (∼3 mm in diameter) dropping on the up- and down-bent surfaces of pristine CNTF and nanoneedle-covered CNTF, respectively. In (e) and (f), we only overlap the images in which the drops maintain their spherical shape to represent the superhydrophobic properties of surfaces. More details can be seen in the movies in the ESI.†

Fig. 2 Microscopic morphology of ZnO nanoneedles. (a) Top-view SEM with low magnification. (b) Side-view SEM. (c) Top-view SEM with high magnification. (d) EDAX result of the region in the red square in (a).

a reaction time of 30 min. Nanoneedles directly grown on the surface of the CNTF are clearly seen in Fig. 2b. The CNTF is the fiber network structure seen below the nanoneedles. However, due to the uneven surfaces of the CNTF, nanoneedles are not as closely packed and straight as those grown on a rigid flat substrate. The average height and tip size of the nanoneedles are 1.5 μm and 20 nm, respectively. As shown in Fig. 2c, there are spiraling steps in the nanoneedles that indicate that their growth mechanism is induced by step climbing of screw dislocations, which is a common growth mechanism for nanoneedles or nanocones. The EDAX results show that these nanoneedles are ZnO.

Subsequently, we characterized the flexibility and superhydrophobicity at the macroscale level. As compared with a pristine CNTF (Fig. 3a), the ZnO–CNTF composite films still maintain their flexibility to be easily bent up and down (Fig. 3b). After modification with fluorosilane, they exhibit excellent superhydrophobicity (inset of Fig. 3b), in contrast to the hydrophobic surfaces of pristine CNTFs (inset of Fig. 3a). Furthermore, we use an injection set to inject macroscale water drops (diameters greater than ~3 mm) on the up- or down-bent surfaces. The overlapped optical images in Fig. 3c–f show

continuous moving trajectories of macroscale water drops. We can clearly see in Fig. 3c and d that surfaces of pristine CNTFs have very high adhesion; hence, when macroscale water drops fall on their surfaces, the drops firmly adhere to the surfaces. In contrast, the surfaces of nanoneedle CNTFs have much lower interfacial adhesion. Fig. 3e and f show that macroscale water drops fall on the nanoneedle surfaces and quickly jump off. Our results verify that the ZnO–CNTF composite films are very robust. Their macroscopic superhydrophobicity is maintained even under continuous up- or down-bent conditions (see the movies in the ESI†).

We take a further step to test the CMDSP functionality of these films. Our studies indicate that the nanoneedle-covered CNT films have the desired CMDSP functionality after fluorosilane modification. Fig. 4a–d show the representative optical top views of the instant self-expulsion process of condensate microdrops on the sample surface. It is evident that the in-plane coalescence of adjacent microdrops, caused by their direct condensation growth, can trigger the out-of-plane jumping of the merged microdrop (as elaborated in Fig. 4e). As shown in Fig. 4g and h, the merged microdrop can eject from the nanosample surface and then fall along a parabolic trajectory. In
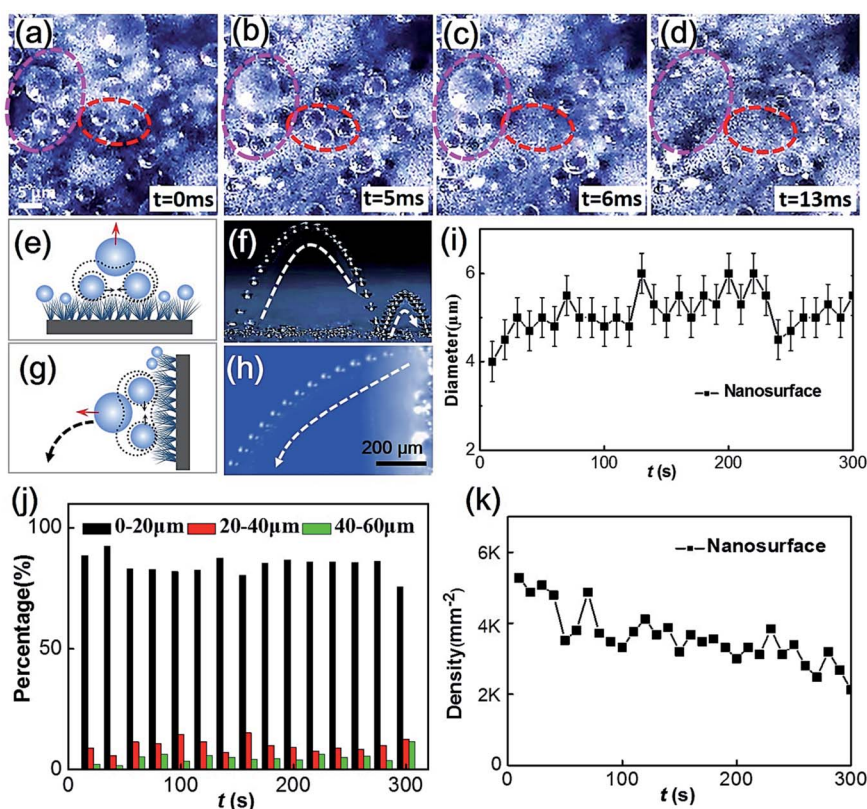
Fig. 4 (a–d) Typical time-lapse optical images showing the self-propelling of condensate microdrops by their mutual coalescence (highlighted by dotted ovals). (e–h) Schematic, overlapped optical top views, and side views showing the coalescence-induced self-jumping of condensate microdrops on horizontal and vertical surfaces, respectively. (i and j) Statistical drop number percentage of condensed microdrops with diameters of <20 μm (black), 20–40 μm (red), and 40–60 μm (green) on the nanostructured surface. Clearly, such a nanostructured film has a remarkable high-density self-renewal ability of small-scale condensate microdrops. The samples are placed on a horizontal or vertical cooling stage with a substrate temperature of approximately 2 °C, ambient temperature of approximately 25 °C, and relative humidity of approximately 85%. (k) Average density per area of condensed microdrops on CMDSP surfaces.
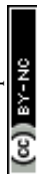
addition, these ejected microdrops can fall back to the sample surface and trigger impact-induced self-propelling events, as shown in Fig. 4f. This CMDSP mode differs from that caused by quasi-static growth and can greatly reduce the residence period of microdrops.

To quantify the self-removal ability of microdrops on the sample surface, we conducted statistical analyses of the diameter (Fig. 4i) and density (Fig. 4k) of condensate drops on the nanostructured surface varied with condensation time, the drop number distribution of residence microdrops with diameters (d) of <20 μm, 20–40 μm, and 40–60 μm (Fig. 4j). Approximately 90% of the microdrops have $d < 20$ μm and have a slight fluctuation with time; around 10% of the microdrops have $d = 20$–40 μm; and almost 4% of the microdrops have $d = 40$–60 μm. The percentage value only increases a little bit with a longer condensation time. Accordingly, the nanoneedle-covered CNT film can realize efficient self-removal of small-scale condensate microdrops, especially those with sizes below 20 μm. It is interesting to note that our CMDSP functionality is far superior even compared with robust and rigid CMDSP surfaces, such as clustered ribbed-nanoneedle structured copper surfaces[23] and porous films of nanoparticles on copper surfaces.[15]

Furthermore, we also bent the composite film to test whether the robust CMDSP functionality is maintained. Fig. 5 shows an optical image of a bent film that was put on an arched ingot's surface. Fig. 5b–e show the CMDSP phenomenon from the top view, indicating that even in the bent parts the CMDSP function is still very robust. Hence, our results indicate that bending does not affect the microscopic superhydrophobicity, and the CMDSP phenomenon is very active and robust on the top of the bent part (as clearly shown in Fig. 5).

We know that the density and height of the ZnO nanoneedle array play an important role in the superhydrophobic CMDSP performances. The construction rules of CMDSP surfaces on rigid metal substrates have been thoroughly discussed in our review paper[1] and recent article.[40] According to previous analyses into the roles of these geometric parameters in governing their CMDSP performance, we know the following basic rules: (1) the increase of tip diameters can lower CMDSP efficiency; (2)

the decrease of interspaces is beneficial to increase CMDSP efficiency; (3) the appropriate height can avoid the easy penetration of moisture. Hence, in this paper, we have constructed the ZnO nanoneedles with optimum parameters mentioned in a previous paper.[40] However, besides following those rules on rigid surfaces, the case of deformation of flexible surfaces should also be considered, and ZnO nanoneedles on flexible surfaces should not be as straight as those on rigid surfaces. This is because flexible films always work in case of deformation. In this paper, we have tested the CMDSP efficiency in case of bending; as shown in Fig. 5, our results show that the CMDSP function can be maintained even when this film is bent. Very recently, Wang *et al.* designed a robust superhydrophobic surface on different types of rigid substrates; the water repellency of the resulting superhydrophobic surfaces is preserved even after abrasion by sandpaper and by a sharp steel blade.[42] Inspired by this work, our study on the improvement of durability of flexible superhydrophobic CMDSP film in real applications is underway.

4. Conclusion

We report the first robust and flexible superhydrophobic surfaces with the desired condensate microdrop self-propelling functionality. This ability may be used to develop CNTF-based flexible surfaces for moisture self-cleaning and anti-frosting behaviors, power generation, electrical energy harvesting, enhanced condensation heat transfer, and conventional superhydrophobicity applications with regard to macroscopic droplets. These low-cost and robust CNTF-based CMDSP surfaces are also suitable for other functional devices, which can advance the development of flexible electronics. Such CNTF-based flexible surfaces are very robust for both macro- and micro-condensation drops, which can be demonstrated by multiple cycles of bending of the film-coated substrate without impacting the surface superhydrophobicity and CMDSP performance. In addition, our method is facile, low-cost, scalable, and has the potential to evolve into practical nano-engineering technologies for CNTF-based surfaces. We plan to further optimize the functional layers and increase the tolerance to mechanical damage. The proposed light and flexible material combined with the CMDSP concept will lead to a novel generation of multifunctional and flexible energy-saving coatings.

Author contributions

X. G. designed the experiments. Z. Y. performed the materials fabrication. J. X. carried out the materials characterization and collected some data. X. G. and S. R. performed analysis of the data. X. G. and S. R. wrote the manuscript.
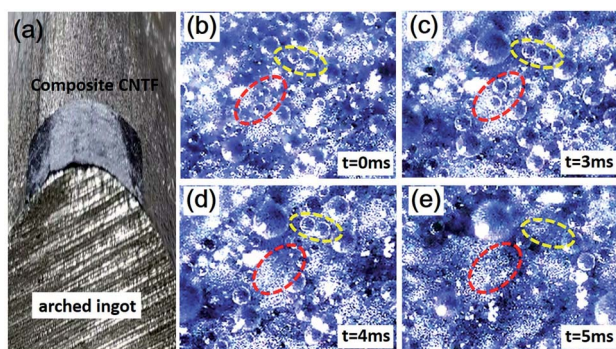

Fig. 5 (a) Optical image of a bent film that was put on an arched ingot's surface. (b–e) Typical time-lapse optical images showing the self-propelling of condensate microdrops by their mutual coalescence (highlighted by dotted ovals).

Conflicts of interest

There are no conflicts to declare.

Acknowledgements

References

1 X. Gong, X. Gao and L. Jiang, *Adv. Mater.*, 2017, **29**, 1703002.

2 Y. Luo, X. Gong, Y. Chen, J. Zhu, J. Wei and X. Gao, *ChemNanoMat*, 2016, **2**, 1018.

3 N. Miljkovic and E. Wang, *MRS Bull.*, 2013, **38**, 397.

4 N. Miljkovic, R. Enright, Y. Nam, K. Lopez, N. Dou, J. Sack and E. Wang, *Nano Lett.*, 2013, **13**, 179.

5 Y. Hou, M. Yu, X. Chen, Z. Wang and S. Yao, *ACS Nano*, 2015, **9**, 71.

6 J. B. Boreyko and C.-H. Chen, *Phys. Rev. Lett.*, 2009, **103**, 184501.

7 F.-C. Wang, F. Yang and Y.-P. Zhao, *Appl. Phys. Lett.*, 2011, **98**, 053112.

8 M. He, X. Zhou, X. Zeng, D. Cui, Q. Zhang, J. Chen, H. Li, J. Wang, Z. Cao, Y. Song and L. Jiang, *Soft Matter*, 2012, **8**, 6680.

9 B. Peng, S. Wang, Z. Lan, W. Xu, R. Wen and X. Ma, *Appl. Phys. Lett.*, 2013, **102**, 151601.

10 C. Lv, P. Hao, Z. Yao, Y. Song, W. Zhang and F. He, *Appl. Phys. Lett.*, 2013, **103**, 021601.

11 C. Feng, L. Wang, J. Chen and Y. Cao, *Macromol. Rapid Commun.*, 2018, **40**, 1800708.

12 N. Miljkovic, D. J. Preston, R. Enright and E. N. Wang, *Appl. Phys. Lett.*, 2014, **105**, 013111.

13 M. Qu, J. Liu and J. He, *RSC Adv.*, 2016, **6**, 59405.

14 J. Feng, Z. Qin and S. Yao, *Langmuir*, 2012, **28**, 6067.

15 Y. Luo, J. Li, J. Zhu, Y. Zhao and X. Gao, *Angew. Chem., Int. Ed.*, 2015, **54**, 4876.

16 Y. Zhao, Y. Luo, J. Li, F. Yin, J. Zhu and X. Gao, *ACS Appl. Mater. Interfaces*, 2015, **7**, 11079–11082.

17 K.-C. Park, H. J. Choi, C.-H. Chang, R. E. Cohen, G. H. McKinley and G. Barbastathis, *ACS Nano*, 2012, **6**, 3789.

18 K. M. Wisdom, J. A. Watson, X. Qu, F. Liu, G. S. Watson and C.-H. Chen, *Proc. Natl. Acad. Sci. U. S. A.*, 2013, **110**, 7992.

19 Y. Zhao, Y. Luo, J. Zhu, J. Li and X. Gao, *ACS Appl. Mater. Interfaces*, 2015, **7**, 11719.

20 Q. Xu, J. Li, J. Tian, J. Zhu and X. Gao, *ACS Appl. Mater. Interfaces*, 2014, **6**, 8976.

21 W. Zhang, G. Lin, J. Li, H. Xue, Y. Luo and X. Gao, *Adv. Mater. Interfaces*, 2015, **2**, 1500238.

22 H. Li, J. Zhu, Y. Luo, F. Yu, J. Fang and X. Gao, *Adv. Mater. Interfaces*, 2016, **3**, 1600362.

23 J. Zhu, Y. Luo, J. Tian, J. Li and X. Gao, *ACS Appl. Mater. Interfaces*, 2015, **7**, 10660.

24 J. Li, Y. Luo, J. Zhu, H. Li and X. Gao, *ACS Appl. Mater. Interfaces*, 2015, **7**, 26391.

25 J. Tian, J. Zhu, H.-Y. Guo, J. Li, X.-Q. Feng and X. Gao, *J. Phys. Chem. Lett.*, 2014, **5**, 2084.

26 C. Dorrer and J. Rühe, *Adv. Mater.*, 2008, **20**, 159.

27 S. Zhang, J. Huang, Y. Tang, S. Li, M. Ge, Z. Chen, K. Zhang and Y. Lai, *Small*, 2017, **13**, 1600687.

28 J. Li, W. Zhang, Y. Luo, J. Zhu and X. Gao, *ACS Appl. Mater. Interfaces*, 2015, **7**, 18206.

29 M.-K. Kim, H. Cha, P. Birbarah, S. Chavan, C. Zhong, Y. Xu and N. Miljkovic, *Langmuir*, 2015, **31**, 13452.

30 J. Feng, Y. Pang, Z. Qin, R. Ma and S. Yao, *ACS Appl. Mater. Interfaces*, 2012, **4**, 6618.

31 R. Wen, Q. Li, J. Wu, G. Wu, W. Wang, Y. Chen, X. Ma, D. Zhao and Y. Yang, *Nano Energy*, 2017, **33**, 177.

32 E. Ölçeroglu, E. Hsieh, M. M. Rahman, K. K. S. Lau and M. McCarthy, *Langmuir*, 2014, **30**, 7556.

33 X. Chen, J. Wu, R. Ma, M. Hua, N. Koratkar, S. Yao and Z. Wang, *Adv. Funct. Mater.*, 2011, **21**, 4617.

34 J. Liu, H. Y. Guo, B. Zhang, S. Qiao, M. Shao, X. Zhang, X. Q. Feng, Q. Li, Y. Song, L. Jiang and J. Wang, *Angew. Chem., Int. Ed.*, 2016, **55**, 4265.

35 S. Liu, X. Zhang and S. Seeger, *ACS Appl. Mater. Interfaces*, 2019, **11**, 44691.

36 Q. Li, H. Liu, S. Zhang, D. Zhang, X. Liu, Y. He, L. Mi, J. Zhang, C. Liu, C. Shen and Z. Guo, *ACS Appl. Mater. Interfaces*, 2019, **11**, 21904.

37 L. Li, Y. Bai, L. Li, S. Wang and T. A. Zhang, *Adv. Mater.*, 2017, **29**, 1702517.

38 L. Gao, L. Chao, M. Hou, J. Liang, Y. Chen, H. Yu and W. Huang, *npj Flexible Electron.*, 2019, **3**, 4.

39 Y.-L. Li, I. A. Kinloch and A. H. Windle, *Science*, 2004, **304**, 276.

40 R. Wang, J. Zhu, K. Meng, H. Wang, T. Deng, X. Gao and L. Jiang, *Adv. Funct. Mater.*, 2018, **28**, 1800634.

41 J. Xu, X. Gong, Z. Yong and S. Ramakrishna, *Mater. Today Chem.*, 2020, **16**, 100253.

42 D. Wang, Q. Sun, M. J. Hokkanen, C. Zhang, F.-Y. Lin, Q. Liu, S.-P. Zhu, T. Zhou, Q. Chang, B. He, Q. Zhou, L. Chen, Z. Wang, R. H. A. Ras and X. Deng, *Nature*, 2020, **582**, 55.